Phase ordering in one-dimensional systems with long-range interactions

Benjamin P. Lee* and John L. Cardy*
Department of Physics, University of California, Santa Barbara, Santa Barbara, California 93106-9530
(Received 24 May 1993)

We study the dynamics of phase ordering of a nonconserved, scalar order parameter in one dimension, with long-range interactions characterized by a power law $r^{-d-\sigma}$. In contrast to higher-dimensional systems, the point nature of the defects allows simpler analytic and numerical methods. We find that, at least for $\sigma > 1$, the model exhibits evolution to a self-similar state characterized by a length scale which grows with time as $t^{1/(1+\sigma)}$, and that the late-time dynamics is independent of the initial length scale. The insensitivity of the dynamics to the initial conditions is consistent with the scenario of an attractive, nontrivial renormalization-group fixed point which governs the late-time behavior. For $\sigma \leq 1$ we find indications in both the simulations and an analytic method that this behavior may be dependent on system size.

PACS number(s): 64.60.Cn, 64.60.My

I. INTRODUCTION

The problem of the dynamical behavior of systems quenched from a disordered phase to an ordered phase has proven to be difficult to solve [1]. At late times the dynamics is described by the motion of domain walls separating equilibrated regions. It is believed that the domain wall morphology is self-similar in time, and characterized by a length scale growing with a power law t^{ρ}. The universal nature of the dynamics has prompted attempts to incorporate a renormalization-group scheme in describing the asymptotically late times [2], and also to determine the various universality classes. The value of ρ appears to depend strongly on the presence or absence of conservation laws, and also on the dimension of the order parameter. Unlike equilibrium critical phenomena, however, the dimension of the system does not play a key role. The generally accepted value for a scalar, nonconserved order parameter (to which we restrict ourselves in this paper) with short-range interactions is $\rho = \frac{1}{2}$ [3,4].

Recent interest has been directed toward including long-range interactions in the systems, characterized by a power law $V(r) \sim -r^{-d-\sigma}$ [5]. Using energy dissipation arguments, Bray and Rutenberg have found the growth law exponent to be modified by the long-range interactions. In particular, they argue that, in the case of the scalar, nonconserved order parameter system, $\rho = 1/(1+\sigma)$ for $\sigma < 1$, and that $\rho = \frac{1}{2}$ with logarithmic corrections for $\sigma = 1$. For $\sigma > 1$, and $d > 1$, they recover the exponent for short-range interacting systems, $\rho = \frac{1}{2}$.

The addition of long-range interactions brings both complication and simplification to the problem. The complication stems from the fact that the local evolution depends on the global state of the system, which makes numerical simulation particularly difficult. However, one simplification is that the presence of long-range interactions allows the possibility of studying one-dimensional systems, since it is known that for $0 < \sigma \leq 1$ the $d = 1$ Ising model has a nontrivial phase transition and thus an equilibrium two-phase region. Also, for higher-dimensional systems long-range forces may dominate the curvature forces, allowing the latter to be neglected. In this paper, however, we restrict ourselves to one-dimensional systems.

The contents of the paper are as follows: in the next section we discuss the model for our system, a continuum Langevin equation without the noise term. We show the equivalence of this model to that of the dynamic Ising model for nonconserved order parameter (Glauber dynamics [6]). In Sec. III we develop an approach based on renormalization-group concepts, and propose a general feature of the dynamics: asymptotic lack of dependence on the initial length scale. We also present numerical data for $\sigma = \frac{1}{2}$ which is in disagreement with the predicted value of $\rho = 1/(1+\sigma)$, and also exhibits dependence on the system size, L. The lack of dependence on the initial length scale and the system size dependence are the principal results of this paper. In Sec. IV we describe a fugacity expansion which leads to direct computation of a Callan-Symanzik-type β function in the large σ limit. When we consider values of $\sigma \leq 1$ we find divergent terms appearing in our expansion, which may be related to the anomalous behavior in the simulations. However, in contrast, the $Q \to \infty$ Potts model has similar divergences, but when simulated seems to give the expected value of $\rho = 1/(1+\sigma)$. In Sec. V we present a method for coupling the dynamics of the density and the two-particle distribution function which leads to qualitatively accurate results. In Sec. VI we discuss our simulation methods, and in Sec. VII we present our conclusions.

II. THE MODEL

In the following section we present a low-temperature mapping from the long-range Ising Hamiltonian with spin degrees of freedom to a Hamiltonian with domain wall degrees of freedom. Next we introduce dynamics to the system via Langevin equations without a noise term.

This is shown to be equivalent to Glauber dynamics when $\sigma \leq 1$. Finally, we discuss related models which are motivated by the simplifications they offer.

A. Ising Hamiltonian

We begin by considering the one-dimensional Ising Hamiltonian

$$H = -J \sum_{\substack{i,j \\ i<j}} s_i s_j V(x_i - x_j) , \tag{1}$$

where

$$V(x_i - x_j) = |x_i - x_j|^{-(1+\sigma)} \tag{2}$$

and the lattice spacing $a = 1$. It is known [7] that this system has a phase transition with some nonzero T_c when $0 < \sigma \leq 1$, and so there is a two-phase equilibrium region for $T < T_c$. Since we are interested in the dynamics of the domain walls, which are point objects in this one-dimensional case, it is convenient to map this Hamiltonian with spin degrees of freedom to one with domain wall degrees of freedom via a lattice equivalent of integration by parts. The resultant Hamiltonian is (apart from surface terms)

$$H = J \sum_{\substack{i,j \\ i<j}} s_i' s_j' U(x_i - x_j) , \tag{3}$$

where the lattice derivatives are defined as $s_i' = s_{i+1} - s_i$, and the function $U(x_i - x_j)$, the lattice equivalent of the second antiderivative of $V(x_i - x_j)$, is defined by

$$V(r) = U(r+1) - 2U(r) + U(r-1) . \tag{4}$$

The boundary conditions are chosen so that $U(r)$ contains no constant or linear pieces, with the solution for $r \gg 1$

$$U(r) = \begin{cases} \dfrac{|r|^{1-\sigma}}{\sigma(1-\sigma)} + O(1/r), & \sigma \neq 1 \\ -\log|r| + O(1/r), & \sigma = 1 . \end{cases} \tag{5}$$

Since the limit of zero lattice spacing is well behaved, and the important contributions from the long-range interactions should be arising at large r, the late-time dynamics of the theory should be unaffected by taking the continuum limit.

The s_i' are zero everywhere neighboring spins are aligned, and equal to ± 2 at the domain boundaries. Therefore the sum over spins can be replaced by a sum over the positions of the domain walls. The sign, or charge, of the domain walls will be alternating, with the consequence that nearest neighbors will attract, next-nearest neighbors will repel, and so on. Absorbing the coupling constant J into a rescaling of the spins, we get the Hamiltonian

$$H = \sum_{\substack{i,j \\ i<j}} (-1)^{i+j} U(x_i - x_j) . \tag{6}$$

B. Dynamical model

To add dynamics to this Hamiltonian we use Langevin-type equations of motion, introducing a kinetic coefficient Γ.

$$\frac{dx_i}{dt} = -\Gamma \frac{\partial H}{\partial x_i} . \tag{7}$$

We neglect any possible noise term, for reasons which we explain below. There is an additional rule to the dynamics. When two charges meet each other they annihilate, and are both removed from the system. In the original spin picture this corresponds to an island of up spins shrinking to zero in a background of down spins, or vice versa.

These equations of motion for the domain walls are equivalent, for $\sigma \leq 1$ and low temperatures, to using Glauber dynamics for the spins [6]. To see this, consider a Glauber dynamical Ising model with temperature β, lattice spacing a, and characteristic free spin flip rate α. The flip rates for interacting spins are found via detailed balance:

$$\frac{w(+)}{w(-)} = \exp(-\beta \Delta E) , \tag{8}$$

where $w(-)$ and $w(+)$ are the rates for flips down and up, respectively, and $\Delta E = E_+ - E_-$ is the energy difference of the spin positions. We are interested in the parameter range where $w(-)$ and $w(+)$ are nearly equal to α, or $\beta \Delta E$ is small. Consider an isolated pair of domain walls separated by distance l as shown in Fig. 1. The domain wall on the left can move through either a spin A flip up or spin B flip down. If we assume that the $w(+)$ in the neighborhood of the domain wall are equal to $w(A+)$, and the $w(-)$ are equal to $w(B-)$, then the motion of the wall will be a random walk superimposed over a slight drift with velocity

$$\begin{aligned} v_d &= a[w(-) - w(+)] \\ &= a w(-)[1 - e^{-\beta \Delta E}] \\ &= a \alpha \beta \Delta E + O((\beta \Delta E)^2) . \end{aligned} \tag{9}$$

The energy difference $\Delta E = J[U(l+a) - U(l)] \simeq aJ(dU/dl)$ if $l \gg a$. If the domain wall position is labeled by x (so $dl/dx = -1$), then the drift velocity equation is

$$\frac{dx}{dt} = -a^2 \alpha \beta J \frac{\partial U}{\partial x} . \tag{10}$$

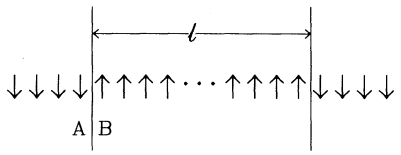

FIG. 1. An isolated pair of domain walls separated by a distance l. The domain wall on the left can move via a flip of spin A or spin B. The difference in the up and down flip rates gives rise to a drift velocity.

This can be generalized to systems of multiple domain walls by considering $U(x-y)$ to be a pairwise interaction energy which carries with it the appropriate sign for attractive and repulsive interactions. By comparison to our original Langevin equations we identify the kinetic coefficient $\Gamma = a^2 \alpha \beta J$.

Thus far we have neglected the possibility of domain wall pair creation. The energy for pair creation at distances of order a is small, and even at low temperatures will occur frequently. However, the energy required to create a pair separated at a macroscopic distance l' is quite large relative to the energy required to move a domain wall a distance a in the presence of another domain wall at l. That is, for large β we can satisfy simultaneously $\beta J U(l') \gg 1$ and $a\beta J(dU/dl) \ll 1$ for finite U, dU/dl. The next question to address is which process, the random walk or the deterministic drift, dominates the dynamics at late times.

The characteristic length of a random walk at time t is

$$l_{\mathrm{RW}} = [(\text{number of steps}) \times a]^{1/2} = (a \alpha t)^{1/2} . \tag{11}$$

Since $\alpha \propto \Gamma T$ then

$$l_{\mathrm{RW}} \sim T^{1/2} t^{1/2} . \tag{12}$$

There is also a length scale determined by the drift velocity which grows with time as

$$l_d \sim t^{1/(1+\sigma)} , \tag{13}$$

which is found from the equations of motion (see Sec. III). The time dependence of these length scales determines which process controls the dynamics. For $\sigma > 1$ we find $l_{\mathrm{RW}} > l_d$ for large t, so a pair of charges can escape annihilation via a random walk. This is the dynamical picture of the disordered phase, as was found in the nearest-neighbor Ising model [8]. For $\sigma = 1$ and $T < T_c$ we find $l_d > l_{\mathrm{RW}}$, which means that a pair of charges can no longer escape annihilation. For $\sigma < 1$ also the drift dominates the dynamics at low temperatures. While this argument would suggest that this is true for all T, it ignores higher-order screening effects which renormalize J, causing the random walk effects to dominate above the critical point. When the drift does dominate, the presence of the random walk should cause at most a finite renormalization of the kinetic coefficient Γ. To summarize, the Glauber model of dynamics is equivalent to the Langevin equations without noise for $\sigma \leq 1$ and $T < T_c$, and otherwise is equivalent to domain walls undergoing random walks.

C. Related models

While $\sigma \leq 1$ is the physically interesting range, the model, without noise, can be extended to values of $\sigma > 1$. If the late-time dynamics is described by some renormalization-group fixed point, then this fixed point might be qualitatively similar for all σ. For example, we find in simulations that, to within our accuracy, the length scale given by the density grows with power law $t^{1/(1+\sigma)}$ for both $\sigma = 1$ and 2. In Sec. IV we show that the dynamical equations simplify in the large σ limit of this model. From this limit we can then work back to study the behavior of models with smaller values of σ.

A similar but more simple system than the Ising model is the Q-state Potts model in the limit of $Q \to \infty$. This model can be mapped to an interacting defect Hamiltonian which has the same power-law interactions as the Ising model, but only between nearest neighbors. All other pairs are noninteracting, which makes this system much easier to simulate on the computer. The annihilation rules are modified as well, in that a pair of defects annihilate to leave behind a single defect. A derivation of the properties of this model is given in Appendix A.

III. SCALING ARGUMENTS AND NUMERICAL RESULTS

A. Initial conditions and scaling functions

The initial conditions for the dynamical system are drawn from some distribution. Measurements of the system, such as the density $n(t)$, or the two-particle distribution function $n_2(r,t)$, are defined to be averaged over this distribution. One could use a thermal distribution corresponding to T_0, the prequench temperature of the system. Instead we use an initial distribution where charges are placed randomly with some initial density n_0, which for $n_0 = (2a)^{-1}$ corresponds to the system being prepared at $T = \infty$ prior to quenching. For values of $n_0 < (2a)^{-1}$ the random distribution is no longer representative of a thermal distribution, but this approach enables us to explore the sensitivity to initial conditions without the complication of initial correlations.

To write scaling functions for the quantities such as the density $n(t)$, we consider all the parameters with dimension in the model. The initial density n_0 gives a length scale, as does the system size L for finite systems. The lattice spacing has been taken to zero. There is one other length scale, given by time. One way to define this length is by the range over which an isolated pair of charges will annihilate in time t. For a pair of charges separated by some distance l the equations of motion can be written as a single differential equation

$$\frac{dl}{dt} = -2\Gamma l^{-\sigma} , \tag{14}$$

which has the solution

$$l(t)^{1+\sigma} = l(0)^{1+\sigma} - 2(1+\sigma)\Gamma t . \tag{15}$$

By setting $l(t) = 0$ we see that the time to annihilation as a function of the initial distance l is

$$t = \frac{1}{2(1+\sigma)\Gamma} l^{1+\sigma} . \tag{16}$$

We rescale the time

$$2(1+\sigma)\Gamma t \to t \tag{17}$$

so that the length scale associated with time is

$$l_t = t^{\zeta} , \tag{18}$$

where

$$\zeta=\frac{1}{1+\sigma} \tag{19}$$

is introduced for notational convenience. This length scale given by t^{ζ}, as well as those of L and n_0^{-1} are the only quantities with dimension in the system. Therefore

$$n(t)=n_0\Phi(n_0t^{\zeta},Lt^{-\zeta}) . \tag{20}$$

Generally it is assumed that the density does not depend on the system size, in which case we get the stronger scaling law

$$n(t)=n_0f(n_0t^{\zeta}) . \tag{21}$$

To determine which of these scaling functions apply, we first turn to numerical simulations (for details, see Sec. VI). By varying the initial number of charges N_0 and system size L such that the initial density n_0 is unchanged, the system size dependence of the model can be directly probed. For $\sigma=2$ these plots superpose, shown in Fig. 2, implying no system size dependence. For $\sigma=1$ we find a slight system size dependence (Fig. 3) wherein the smaller systems drop below the scaling curve at late t.

We also measure the time dependence of the density for $\sigma=2$, and find that it is consistent with the $\sigma<1$ prediction of $n(t)\sim t^{-\zeta}$ for large t [5]. This result and the scaling form of the density (21) have the corollary that $n(t)$ is independent of n_0. That is, since $f(x)=Ax^{-1}$ for large x, then

$$n(t)\sim n_0\frac{A}{n_0t^{\zeta}}=At^{-\zeta} . \tag{22}$$

We can plot the same data shown in Fig. 2, but rescaled so all the runs have the same system size, but different initial densities. In Fig. 4 we see that the plots converge to the same function asymptotically. We propose that the lack of dependence on the initial length scale may be a general feature of the late-time dynamics. This is suggestive of T_0 independence for initial conditions corresponding to thermal distributions.

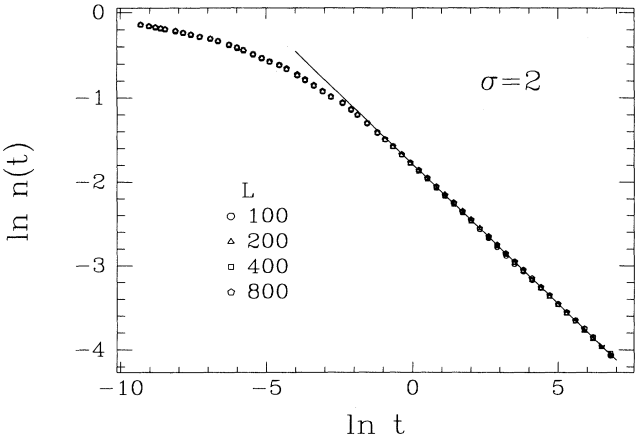

FIG. 2. Simulations for $\sigma=2$, shown on a log-log plot. The system sizes used are $L=100$, 200, 400, and 800, and the initial density is fixed at $n_0=1$. The data show no system size dependence. The power law $n\sim t^{-1/3}$ is plotted as a visual reference, and is in good agreement with the data. The error bars for the data are smaller than the points plotted.

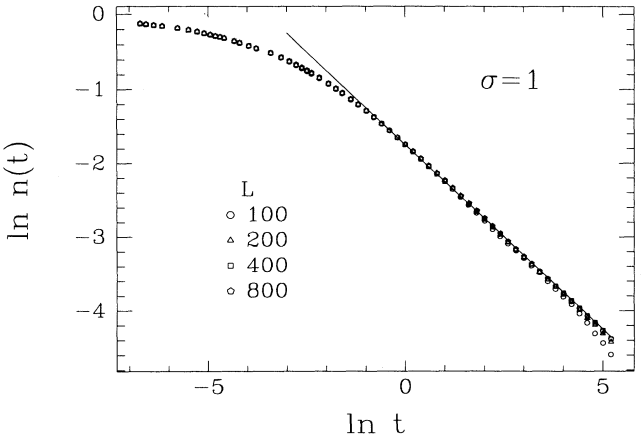

FIG. 3. Simulations for $\sigma=1$. The same range of system sizes is used as in Fig. 2. The data for smaller L values exhibit slight system size dependence. The power law $n\sim t^{-1/2}$ is plotted as a visual reference. The statistical error bars are smaller than the points plotted.

B. Renormalization-group approach

The dynamics of the system, for $\sigma=2$ at least, appears to be scale invariant at late times. That is, evolving the system from time t_1 to t_2, where both times are chosen from the late-time region, is the same as rescaling the system at t_1 by a factor of

$$b=\left[\frac{t_2}{t_1}\right]^{\zeta} . \tag{23}$$

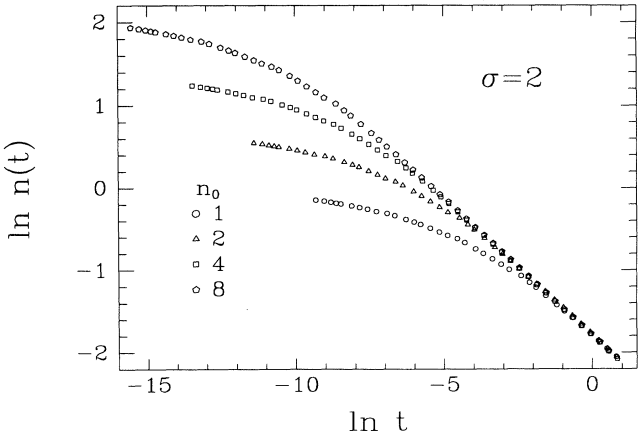

FIG. 4. The same data for $\sigma=2$ as shown in Fig. 2, but rescaled so that $L=100$ and the initial density $n_0=1$, 2, 4, and 8. The curves collapse to a single function, implying the system is independent of the initial density at late times.

Stated another way, the time-dependent domain wall probability distribution is invariant under a rescaling of the system that includes the length scale of time (but not the initial length scale). The numerical data for the density is consistent with this presumed scale invariance, since $n(t)=At^{-\zeta}$ is preserved under rescaling $n\to n/b$ and $t\to tb^{1/\zeta}$.

This scale invariance motivates an analogy to a second-order critical point in equilibrium statistical mechanics, where renormalization-group (RG) methods are applicable [9]. The general RG approach is a two-step process. First one integrates out the short distance behavior of the system from some cutoff a to ba, creating an effective theory with modified coupling constants. Second, one rescales the system by the factor b, restoring the original value of the cutoff. The behavior of the coupling constants under this transformation determines the renormalization flow of the theory. The analog of integrating out the short-distance behavior is evolving the system forward in time [2]. The system is then rescaled back to the original point in time, giving a modified theory. When the system reaches the point where it is invariant under this transformation, it has reached a stable, self-similar state in which it will remain for $t\to\infty$.

To describe the flow of the theory to its fixed point we define a Callan-Symanzik β function [10]. First we define the renormalized coupling as the density at an arbitrary but fixed late time τ. This is the analog of the normalization point. The dimensionless coupling constant, which will be invariant under rescaling, is then

$$g_R=(\Gamma_R\tau)^{\zeta}n(\tau)\ . \tag{24}$$

We have restored the time constant Γ in the problem, since it is possible that renormalization effects may cause an effective time dependence in Γ_R. This will be discussed at the end of Sec. IV. For the purposes of the present argument we will assume that Γ is a constant and can be absorbed into a rescaling of time. A late-time correlation function of the system can be expressed either in terms of the random initial state evolved in time, or from the normalization point where the initial state information has been lost. That is, for some correlation function $G(r,t)$ we have

$$G(r,t,n_0)=G_R(r,t,g_R,\tau)\ . \tag{25}$$

The value of G is independent of the normalization scale, so

$$\tau\frac{\partial}{\partial\tau}G\bigg|_{r,t,n_0}=0\ , \tag{26}$$

which implies a Callan-Symanzik equation

$$\left[\tau\frac{\partial}{\partial\tau}+\beta(g_R)\frac{\partial}{\partial g_R}\right]_{r,t,n_0}G_R=0\ , \tag{27}$$

where

$$\beta(g_R)=\tau\frac{\partial g_R}{\partial\tau}\bigg|_{r,t,n_0}\ . \tag{28}$$

If G_R has dimensions (length)^n, then dimensional analysis gives

$$\left[-n+\frac{\tau}{\zeta}\frac{\partial}{\partial\tau}+\frac{t}{\zeta}\frac{\partial}{\partial t}+r\frac{\partial}{\partial r}\right]_{g_R}G_R(r,t,g_R,\tau)=0\ . \tag{29}$$

Combining (27) and (29) to eliminate the explicit τ dependence gives

$$\left[n-\frac{t}{\zeta}\frac{\partial}{\partial t}-r\frac{\partial}{\partial r}+\beta(g)\frac{\partial}{\partial g}\right]G_R=0\ . \tag{30}$$

If $\beta(g_R^*)=0$ for some value of the dimensionless coupling g_R^*, then

$$G_R=r^n h(rt^{-\zeta})\ , \tag{31}$$

which is the self-similar fixed point. Also, for $g_R(\tau)=g_R^*$ we find

$$n(t)=g_R^* t^{-\zeta}\ , \tag{32}$$

the asymptotic form of the density predicted in the energy dissipation arguments. The flow into this fixed point for a given set of initial conditions is determined by the β function. We stress that in this formalism the assumption of a zero of β is mathematically completely equivalent to the statement that $n(t)t^{\zeta}\to$const, but it gives a conceptually different approach to the problem, and from an approximation standpoint, a method for extrapolating from the early- to the late-time regime. In Sec. IV we will discuss a method for finding the β function in the large σ limit.

C. Anomalous behavior for $\sigma=\frac{1}{2}$

For the case of $\sigma=\frac{1}{2}$ we find that the expected power-law behavior of $n(t)\sim t^{-\zeta}$ is not observed. The simulations, shown in Fig. 5, exhibit less than convincing

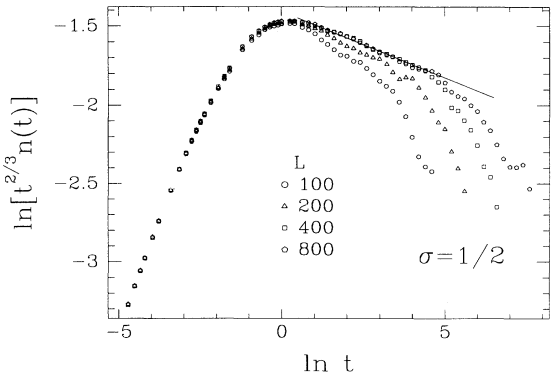

FIG. 5. Simulations for $\sigma=\frac{1}{2}$. The initial density is fixed at $n_0=1$, and the system size varies from $L=100$ to 800. On the vertical axis is plotted $\ln(t^{2/3}n)$, which should be a constant in the scaling regime. The data show strong system size dependence, and no range over which the density has the expected $t^{-2/3}$ power-law dependence. The line drawn represents $n\sim t^{-0.75}$. The error bars for the $L=800$ data are smaller than the size of the points plotted up to $\ln t=4$.

power-law behavior, and the density decays with an exponent of at least $-\rho=-0.75$. From the scaling forms (20) and (21) it follows that this implies either a dependence on n_0 at late times, or dependence on the system size L, or both. The data indicate a fairly strong L dependence.

These simulations are quite difficult. We attempted to reproduce periodic boundary conditions by including interactions wrapped around the system, up to some long-range cutoff. For $\sigma=\frac{1}{2}$ the system is more sensitive to the cutoff than in the previous cases, and requires inclusion of many more replicas to simulate periodic boundary conditions (for a discussion of our methods see Sec. VI). We were unable to average over as many realizations of the system, and as a consequence the statistical error bars in the numerical results are appreciable toward the later times. The data are too imprecise to determine whether the system is independent of the initial density, as was shown for $\sigma=2$ in Fig. 2.

We now present a heuristic argument for the lack of dependence on the initial density, which holds even when the system shows L dependence. Consider a system which has evolved some very short time δt. Then

$$n(\delta t)=n_0\Phi(n_0\delta t^{\zeta},\delta t^{\zeta}/L) \\ =n_0-2n_0^2\delta t^{\zeta}+O(\delta t^{2\zeta}) , \quad (33)$$

where $x=n_0t^{\zeta}, y=t^{\zeta}/L$, and the coefficient of the δt^{ζ} term, $\partial\Phi(0,0)/\partial x=2$, is found in Sec. IV. Also in Sec. IV we show that there can be no L dependence until at least order n_0^3, so $\partial\Phi(0,0)/\partial y$ is zero. In this short time δt the system will build up correlations, but primarily at short distances. This short-distance information is quickly leaving the system via annihilation. We assume that although there are long-distance correlations building up, they, nevertheless, depend on only one length scale, given by $n(t)$. This assumption is expressed in terms of (20) by taking $n_0\to n(\delta t)$ and $t\to t-\delta t$, so that

$$n_0\Phi(n_0t^{\zeta},t^{\zeta}/L) \\ =n(\delta t)\Phi(n(\delta t)(t-\delta t)^{\zeta},(t-\delta t)^{\zeta}/L) . \quad (34)$$

If we expand the right-hand side of the equation to order δt^{ζ} ($\zeta<1$) then

$$n(t)=n_0\Phi-2\delta t^{\zeta}n_0^2\Phi-2\delta t^{\zeta}n_0^2x\frac{\partial\Phi}{\partial x} . \quad (35)$$

Setting the $O(\delta t^{\zeta})$ term to zero gives the differential equation

$$x\frac{\partial\Phi}{\partial x}=-\Phi , \quad (36)$$

which has the solution

$$\Phi(x,y)\sim g(y)x^{-1} . \quad (37)$$

This argument predicts that the late-time behavior will exhibit lack of dependence on n_0, even though it may depend on L through $g(y)$. The form of the function $g(y)$ is unspecified, and may play a direct role in the asymptotic time dependence.

The original argument which led to Eq. (34) is difficult to make rigorous. The result of the calculation can only be true for asymptotically late times. The short-distance correlations take some time to leave the system before the long-distance correlations dominate the dynamics.

We have also simulated the $Q\to\infty$ Potts model for values of $\sigma=\frac{1}{2}$ and 2, and found that the naive result $n\sim t^{-\zeta}$ is consistent with the data for both values of σ. The data are shown in Fig. 6. One might expect to see different behavior from the Ising system, since in the Potts case there is no need to include multiple wrappings in the interactions. For periodic boundary conditions the only requirement is to include the interaction between the first and last charge.

IV. FUGACITY EXPANSION

A technique for calculating the density $n(t)$ and other correlation functions as expansions in powers of the initial density n_0 is developed in this section, and this result is used to calculate the β function defined in Sec. III to order g_R^4, from which we estimate the fixed point coupling g_R^*.

A. Machinery

We can use the ideas of equilibrium statistical mechanics to calculate quantities which are averages over the distribution of initial conditions. In doing so it is necessary to use finite systems, although at the end of the calculation the $L\to\infty$ limit may be taken, if it exists. The canonical ensemble, with a fixed initial density, is too difficult to work with, so instead we use the fixed fugacity or grand canonical ensemble. One can check afterwards that the fluctuations in the grand canonical ensemble are of order $1/\sqrt{L}$. The average of some quantity is calculated by expanding in powers of the fugacity y. The coefficient of the y^k term is given by the integral of this quantity over all the initial conditions for the k-body sys-

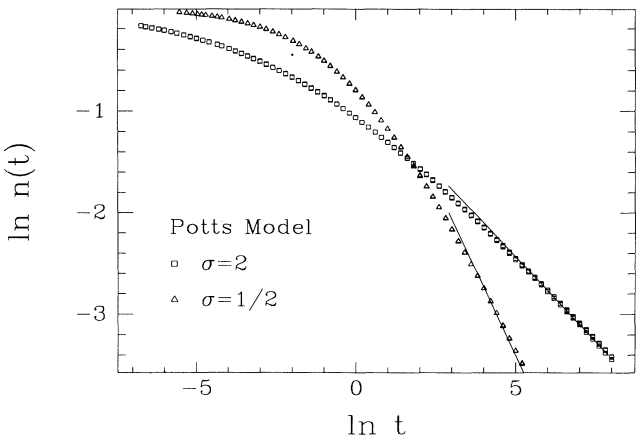

FIG. 6. Simulations of the $Q\to\infty$ Potts model for $\sigma=\frac{1}{2}$ and 2. The lines for both data sets correspond to the $n\sim t^{-\zeta}$ curves. For both values of σ the initial density $n_0=1$ and the system sizes $L=100$, 300, and 1000 are used. The data superpose very well for the different system sizes.

tem. To normalize these averages we use the analog of the grand canonical partition function

$$\Xi=\sum_k y^k V_k \ , \tag{38}$$

where V_k is just the volume of configuration space for the k-body system. We will work with ordered charges, so this volume is $V_k=L^k/k!$. From this it follows that

$$\Xi=e^{yL} \ . \tag{39}$$

The initial number of charges can be found in terms of the fugacity, since the value of N_0 for a k-body system is just k.

$$\begin{aligned} N(0)&=\Xi^{-1}\sum_k y^k k\frac{L^k}{k!} \\ &=yLe^{-yL}\sum_k \frac{(yL)^{k-1}}{(k-1)!} \\ &=yL \ . \end{aligned} \tag{40}$$

Therefore the fugacity is equal to the initial density n_0.

The calculations are actually simpler for a nonperiodic system. It is then important to comment on the boundary conditions, that is, the values of the spins at $x=0$ and L. The spin degeneracy factor of 2 can be ignored, leaving as the possible boundary conditions either the spins at each end being equal, or being opposite. These correspond, respectively, to there being an even or odd number of charges in the system. For convenience, we sum over both cases, corresponding to free boundary conditions on the Ising spins.

We can use the fugacity expansion to calculate the time-dependent number of charges $N(t)$. First we define $N_k(x_1,\ldots,x_k,t)$ to be the number of charges that remain at time t, given k charges at $t=0$ with initial positions $x_1,x_2,\ldots,x_k$. For regions of the configuration space of initial conditions where no annihilation has occurred by time t, $N_k(t)=k$. For regions where exactly one annihilation has occurred by time t, $N_k(t)=k-2$. This continues down to regions where $N_k(t)=0$ or 1, after which no more annihilation is possible. Integrating $N_k(t)$ over the distribution of initial conditions gives the coefficient of the y^k term in the fugacity expansion, which we define to be $Q_k(t)$. That is,

$$Q_k(t)=\int_{0<x_1<\cdots<x_k<L}\prod_{i=1}^{k} dx_i N_k(x_1,\ldots,x_k,t) \ . \tag{41}$$

Calculating $Q_k(t)$ for the random distribution is then a process of partitioning the volume in configuration space by the number of charges at time t, and then summing these regions weighted by their respective charge numbers.

In general the division of configuration space at time t into regions of k, $k-2$, etc. charges requires solving the k-body problem given by our equations of motion. The two-body problem can be solved for all σ, and was found in the preceding section and used to rescale time t. We can use this result to calculate $Q_2(t)$ for general σ [note that $Q_1(t)=L$ for all t]. As defined

$$Q_2(t)=\int_{0<x_1<x_2<L} dx_1 dx_2 2\Theta(x_2-x_1-t^{\zeta}) \ , \tag{42}$$

that is, there is a contribution of 2 from regions of the integral where $x_2(0)-x_1(0)$ is greater than the annihilation distance given by t, and a contribution of zero from the rest, with Θ being the Heaviside step function. The integration variables are the *initial* positions of the particles. The time dependence is explicit in the integrand. Integrating gives

$$Q_2(t)=L^2-2Lt^{\zeta}+t^{2\zeta} \ . \tag{43}$$

This allows us to calculate $n(t)$ to order y^2. Expanding $\Xi^{-1}=e^{-yL}$ to order y gives

$$\begin{aligned} N(t)&=(1-yL)(0+yL+y^2L^2-2y^2Lt^{\zeta}+y^2t^{2\zeta}) \\ &\quad +O(y^3) \\ &=Ly(1-2yt^{\zeta})+O(L^0,y^3) \ . \end{aligned} \tag{44}$$

Dividing both sides by L and taking the $L\to\infty$ limit (or just considering $L\gg t^{\zeta}$) gives

$$n(t)=n_0[1-2n_0t^{\zeta}]+O(n_0^3t^{2\zeta}) \tag{45}$$

or, from (21),

$$f(x)=1-2x+O(x^2) \ . \tag{46}$$

B. Large σ calculation

The higher-order terms become quite difficult. We can solve the three-body system for $\sigma=1$ (see Appendix B), but in general some simplification is needed to proceed. By taking the large σ limit the equations of motion effectively decouple, and we can solve for the higher-order terms. As stated earlier, this limit merits consideration since the value of σ seems to play only a minor role in the nature of the fixed point which characterizes the late times, at least for $\sigma>1$. For the three-body case the equations of motion can be reduced to two equations by introducing the variables $r_i=x_{i+1}-x_i$. In terms of r_1,r_2 the equations of motion are

$$\begin{aligned} \dot{r}_1&=-2r_1^{-\sigma}+r_2^{-\sigma}+(r_1+r_2)^{-\sigma} \ , \\ \dot{r}_2&=-2r_2^{-\sigma}+r_1^{-\sigma}+(r_1+r_2)^{-\sigma} \ . \end{aligned} \tag{47}$$

Now suppose $r_1<r_2$. In the large σ limit the equation of motion for r_1 becomes

$$\dot{r}_1=-2r_1^{-\sigma} \tag{48}$$

and the charges have decoupled. More exactly, the closest pair moves together and annihilates in a time that is infinitely smaller than the time scales of the rest of the charges. With these simplified dynamics we are able to calculate the higher-order terms.

For the $k=3$ case we divide our configuration space into two regions corresponding to the order in which the charges annihilate: $r_1<r_2$ so x_1,x_2 annihilates first, or $r_1>r_2$ so x_2,x_3 annihilates first. The equations of motion are symmetric with respect to r_1 and r_2, so we

can consider just one of these conditions, say $r_2 > r_1$, and double the resulting calculation. We have

$$Q_3(t) = 2\int_{0<x_1<x_2<x_3<L} d^3x\, \Theta(r_2 - r_1) \times [3\Theta(x_2 - x_1 - t^\zeta) + \Theta(t^\zeta - x_2 + x_1)] . \quad (49)$$

We can rewrite the term in square brackets as $3 - 2\Theta(t^\zeta - x_2 + x_1)$. To evaluate this integral it is convenient to take the derivative with respect to t^ζ, which turns the Θ function into a δ function.

$$\frac{\partial Q_3(t)}{\partial t^\zeta} = 2\int_0^L dx_3 \int_0^{x_3} dx_2 \int_0^{x_2} dx_1 \Theta(x_3 - 2x_2 + x_1) \times (-2)\delta(t^\zeta - x_2 - x_1) = -2L^2 + 8Lt^\zeta - 8t^{2\zeta} . \quad (50)$$

Integrating this we get

$$Q_3(t) = \frac{L^3}{2} - 2L^2 t^\zeta + 4Lt^{2\zeta} - \frac{8}{3}t^{3\zeta} , \quad (51)$$

where the constant of integration is given by the $t=0$ value, $Q_k = kL^k/k!$.

To calculate the $k=4$ integral we divide the configuration space into three regions, distinguishable by which pair annihilates first: (1,2), (2,3), or (3,4). By symmetry the first and last cases give identical contributions to the integral. The next step in evaluating the integral is to take the derivative $\partial Q_4/\partial L$. The L dependence of the integral is contained in the $\Theta(L - x_k)$ term implicit in the limits of integration. The L derivative replaces this Θ function with a $\delta(L - x_k)$, against which we can integrate x_k. The remaining $k-1$ integrals over the x_i are changed to integrals over r_i with the constraints $\sum_{i=1}^{k-1} r_i < L$ and $r_i > 0$. Then

$$\frac{\partial Q_4(t)}{\partial L} = \int_{r_1+r_2+r_3<L} dr_1 dr_2 dr_3 [2\Theta(r_3 - r_1)\Theta(r_2 - r_1)\{2\Theta(r_1 - t^\zeta) + 2\Theta(r_3 - t^\zeta)\} + \Theta(r_3 - r_2)\Theta(r_1 - r_2)\{2\Theta(r_2 - t^\zeta) + 2\Theta(r_1 + r_2 + r_3 - t^\zeta)\}] . \quad (52)$$

By taking the t^ζ derivative as before, the integral can be done fairly straightforwardly, with the result

$$\frac{\partial^2 Q_4(t)}{\partial t^\zeta \partial L} = -3L^2 + 14Lt^\zeta - \frac{58}{3}t^{2\zeta} . \quad (53)$$

Integrating this we get

$$Q_4(t) = \frac{L^4}{6} - L^3 t^\zeta + \frac{7}{2}L^2 t^{2\zeta} - \frac{58}{9}Lt^{3\zeta} + \text{const} \times t^{4\zeta} , \quad (54)$$

where again the initial value of Q_4 is used to find the constant of integration. The unknown function of t is proportional to $t^{4\zeta}$, with a proportionality constant which could be calculated by evaluating the integral without the L derivative.

On the basis of the scaling relation (21) one might think that the only piece of the y^k integral that is of interest is the $t^{(k-1)\zeta}$ term. In this case we could take $k-1$ derivatives with respect to t^ζ and then evaluate the remaining integral for $t=0$, a considerable simplification. However, it turns out that all the pieces from lower-order terms, and not just the $t^{(k-1)\zeta}$ piece, feed back into the calculation of higher-order terms. This is a consequence of boundary effects introduced by working with a nonperiodic system. Writing a more careful scaling form for $N(t)$ where both t and L are finite we get

$$N(t) = Lyf(yt^\zeta) + g(yt^\zeta) , \quad (55)$$

where f is the original scaling function, and g some function which corresponds to our choice of boundary conditions. Writing $f(x) = \sum_i f_i x^i$ and $g(x) = \sum_i g_i x^i$, we find

$$\sum_k y^k Q_k(t) = N(t)e^{yL} = Ly(1 + f_1 y t^\zeta + f_2 y^2 t^{2\zeta} + f_3 y^3 t^{3\zeta})e^{yL} + (g_0 + g_1 y t^\zeta + g_2 y^2 t^{2\zeta} + g_3 y^3 t^{3\zeta} + g_4 y^4 t^{4\zeta})e^{yL} + O(y^5 t^{4\zeta}) . \quad (56)$$

The coefficients for f and g can be determined by comparing powers of y on each side of the equation. In general, extracting the coefficient f_k from the $(k+1)$-body integral requires knowing all the g_i for $i \le k$. To order y^4 we find that $g(x) = x^2 - (\frac{8}{3})x^3 + O(x^4)$ and

$$f(x) = 1 - 2x + 3x^2 - \tfrac{34}{9}x^3 + O(x^4) . \quad (57)$$

This density expansion is the main result of this calculation.

With a systematic expansion for the scaling function (21) we have equivalently an expansion for the β function defined by (24) and (28) in powers of g_R. Since $g_R(x) = xf(x)$,

$$\sigma\beta = x\frac{d}{dx}g_R(x) = x - 4x^2 + 9x^3 - \frac{136}{9}x^4 + O(x^5) . \quad (58)$$

To find $\beta(g_R)$ we invert the series $g_R(x)$, which gives

$$\sigma\beta(g_R) = g_R - 2g_R^2 - 2g_R^3 - \tfrac{10}{3}g_R^4 + O(g_R^5) . \quad (59)$$

The fixed point value of g_R if β is truncated at the fourth order is $g_R^* = 0.33$. Truncating to third order would give $g_R^* = 0.37$, a 10% difference. The value of g_R^* is the amplitude A in the asymptotic form of the density

$$n(t) \sim A t^{-\zeta} . \tag{60}$$

This number should be universal in that all systems with the same value of σ (but different n_0) will have the same amplitude. We suspect only a weak σ dependence of this number for values of $\sigma > 1$. The amplitude found from the numerical data for both $\sigma = 1$ and 2 is $A = 0.31$.

C. $\sigma \leq 1$ calculation

While this approach of calculating the large σ terms may give a description of the fixed point, our real goal is to work with values of σ which lie in the range of physical interest. The two-body solution is known for all values of σ. For the three-body term the relevant calculation is the time to the first annihilation, $T(r_1, r_2)$. In the large σ limit this was just given by $T = \min(r_1, r_2)^{1+\sigma}$. For finite σ the presence of the third charge will affect the annihilation of the first and second charges, and always in the direction of slowing down the process. This slowing down will be a maximum when r_1 and r_2 are approximately equal. In Fig. 7 curves of constant T are plotted in the plane of initial conditions r_1, r_2. The curve for the large σ limit is given by vertical and horizontal lines, while the $\sigma = 1$, constant T curve lies to the left and below. For any value of σ the area bounded by the corresponding constant T curve is proportional to $\partial Q_3(t)/\partial L$, as can be seen by writing out the integral

$$\frac{\partial Q_3(t)}{\partial L} = -2 \int_{r_1 + r_2 < L} dr_1 dr_2 \Theta(t - T(r_1, r_2)) . \tag{61}$$

Finding $Q_3(t)$ for $\sigma = 1$ is then a matter of finding the area between the $T(r_1, r_2) = t$ curves for the large σ limit and $\sigma = 1$.

For $\sigma = 1$ an exact solution for $T(r_1, r_2)$ can be found, the details of which are given in Appendix B. The result,

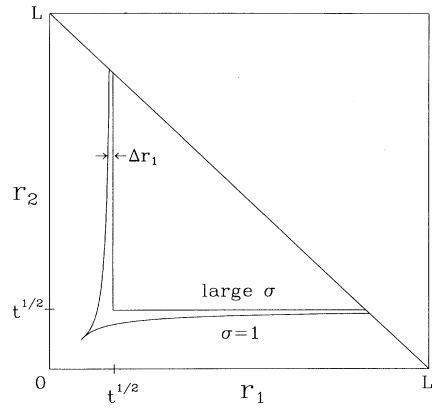

FIG. 7. Curves of constant time to annihilation, $T(r_1, r_2) = t$, in the (r_1, r_2) plane for $\sigma = 1$ and the large σ limit. The area bounded by these curves, the axes, and the line $r_1 + r_2 = L$ gives $\partial Q_3(t)/\partial L$, as shown in the text. The contribution to the area between the $\sigma = 1$ and large σ curves from the asymptotic region is divergent as $L \to \infty$. This can be shown by integrating $\Delta r_1(r_2, t)$ out to $r_2 = L$.

however, gives an area between the two curves which diverges as $L \to \infty$. This is a general feature which occurs for all $\sigma \leq 1$, which can be understood by examining the equations of motion. Consider a three-charge configuration where one separation distance, say r_2, is much larger than the other. The equation of motion for the closer pair is then

$$2(1+\sigma)\dot{r}_1 = -2 r_1^{-\sigma} \left[1 - \frac{r_1^\sigma}{r_2^\sigma} + O\left[\frac{r_1^{2\sigma}}{r_2^{2\sigma}} \right] \right] , \tag{62}$$

where the factor multiplying the left-hand side is a consequence of our rescaling of time in (17). We treat r_2 as a constant in the equation, and integrate the dynamical variable r_1 from its initial value to zero,

$$-\frac{1}{(1+\sigma)} \int_0^T dt = \int_{r_1}^0 dr \left[r^\sigma + \frac{r^{2\sigma}}{r_2^\sigma} + O\left[\frac{r^{3\sigma}}{r_2^{2\sigma}} \right] \right] . \tag{63}$$

This gives $T(r_1, r_2)$ in the asymptotic region described. Performing the integral and inverting to find $r_1(T, r_2)$ gives

$$r_1(T, r_2) = T^\zeta - \frac{T}{(1+2\sigma) r_2^\sigma} + O\left[\frac{T^{\zeta(1+2\sigma)}}{r_2^{2\sigma}} \right] . \tag{64}$$

The first term is just the large σ solution, so the second term gives the leading contribution to $\Delta r_1 = r_1^{(\infty)} - r_1^{(\sigma)}$. Integrating $\Delta r_1(r_2)$ out to $r_2 = L$ gives the area contained in the asymptotic approach to the constant T line of the large σ limit. For $\sigma = 1$ this piece gives $\log L$, and for smaller values of σ it gives an $L^{-1+\sigma}$ term. The significance of the divergences is that they will not cancel when the fugacity expansion is summed, as all the other L-dependent terms do. For $\sigma > 1$ the area remains finite as $L \to \infty$, and so the calculation for $\sigma > 1$ should result in the same terms as in the case of the large σ limit, but with modified coefficients.

It is possible that there may be an infinite set of logarithms (for $\sigma = 1$) which can be summed to restore the intensive behavior of the density. Such a summation may then be used, as in conventional critical dynamics [11], to renormalize the kinetic coefficient Γ, effectively making Γ_R a time-dependent quantity. While this would imply no system size dependence and the density scaling form (21), the time dependence of Γ_R would give rise to anomalous time dependence for the density, as can be seen by (24). This anomalous time dependence carries with it the implication that late-time dynamics will exhibit dependence on the initial density.

An alternate possibility is that these divergent terms are indicating that the asymptotic dynamics truly has system size dependence. If the system were still independent of the initial density, as suggested by our heuristic argument in Sec. III, then this system size dependence would give rise to anomalous time dependence, as can be seen by the scaling function (20). It is worth noting that if there is system size dependence, we can no longer except our calculations, which are performed with free boundaries, to correspond directly to simulations with periodic boundary conditions.

It is possible that both of these effects, system size dependence and a time-dependent Γ_R, occur. The simulations for $\sigma=\frac{1}{2}$, as discussed in Sec. III, are not decisive on this issue, although they do seem to indicate at least the former.

By studying a related model we might hope to find more clues for the significance of the divergences in the fugacity expansion. The $Q\to\infty$ Potts model provides a contrast which further confuses the problem. In the Ising case the divergences were caused by a three-body effect where the annihilation of a close pair, say (x_1,x_2), is slowed by a distant charge, x_3. In the Potts case the distant charge is still interacting with the nearest neighbor, x_2, but not with the charge at x_1. This will give exactly half of the divergent effect seen in the Ising case. However, the simulations show no system size dependence, to within our accuracy.

There is a difference between the two models in the higher-order divergent terms. Presumably the four-body term in the Ising case will have divergent pieces when one of the end charges, say x_4, is distant, and is affecting both of the possible annihilations: (x_1,x_2) and (x_2,x_3). In the $Q\to\infty$ Potts case, the distant charge can only affect the annihilation of the pair which contains the nearest neighbor of the distant charge, in this case (x_2,x_3). However, a quantitative analysis of this effect at higher orders is difficult.

V. TRUNCATION SCHEME FOR THE TWO-PARTICLE DISTRIBUTION FUNCTION

The fugacity expansion provides an exact scheme for calculating time-dependent quantities in the system via the deterministic equations of motion. A simpler scheme can be developed which gives a qualitative description of the scaling regime, and of other features of the model. In this section we will present this method, and discuss the applicability for some different initial conditions.

The two-particle distribution function for the system, $n_2(r,t)$, can be used to find a dynamical equation for $n(t)$. Integrating the distribution function from $r=0$ to δr gives the density of charge pairs which are within δr of each other. For very small separations the charge pairs will become isolated from the rest of the system, and annihilate in a time $\delta t=\delta r^{1/\zeta}$. Therefore the rate of change of the density is given exactly by

$$\frac{dn}{dt}=\lim_{\delta t\to 0}-\frac{2}{\delta t}\int_0^{\delta t^{\zeta}} n_2(r,t)dr \ . \tag{65}$$

The distribution function can be calculated by the fugacity expansion described in the last section. The leading-order term is the two-body term, which can be written

$$n_2(r,t)\propto y^2\int_{r(0)<L} dr(0)\delta(r(t)-r) \ . \tag{66}$$

A change of integration variables from $r(0)$ to $r(t)$ will introduce the Jacobian

$$J(r,t)=\left.\frac{dr(0)}{dr(t)}\right|_{r(t)=r}=\frac{r^{\sigma}}{(r^{1+\sigma}+t)^{\sigma/(1+\sigma)}} \ , \tag{67}$$

which has the limit $J=1$ for $r\to\infty$ or $t=0$. Therefore the distribution function is

$$n_2(r,t)=n_0^2 J(r,t)+O(n_0^3) \ . \tag{68}$$

Notice that the dynamics produces a "hole" in the two-particle distribution function at short distances.

This expansion is only useful for low densities or early times. However, we can extend the range via a heuristic argument similar to that of Sec. III. For an isolated pair of charges separated by a distance r at time $t+\delta t$, the separation at time t is given by $(r^{1+\sigma}+\delta t)^{\zeta}$. Therefore, for small r we expect the two-particle distribution functions of the arguments above to be related. The relation should also include the Jacobian, for the same reason it enters into the $t=0$ calculation. Therefore

$$n_2(r,t+\delta t)=J(r,\delta t)n_2((r^{1+\sigma}+\delta t)^{\zeta},t) + (\text{higher-order terms}) \ . \tag{69}$$

This equation should be exact in the small r limit, and the higher-order terms are corrections for large r. The contributions from the higher-order terms can be approximated by replacing $n_2(r,t)$ with $\bar{n}_2(r,t)=n_2(r,t)/n(t)^2$, so that $\bar{n}_2(r\to\infty,t)=1$. This results in a truncation scheme for $\bar{n}_2$ which is correct both for small r and in the $r\to\infty$ limit. Making this substitution and equating the order δt terms in (69) gives the differential equation

$$\frac{\partial\bar{n}_2}{\partial t}=-\left[\frac{\sigma}{1+\sigma}\right]\frac{\bar{n}_2}{r^{1+\sigma}}+\left[\frac{1}{1+\sigma}\right]\frac{1}{r^{\sigma}}\frac{\partial\bar{n}_2}{\partial r} \tag{70}$$

whose general solution is

$$\bar{n}_2(r,t)=r^{\sigma}g((r^{1+\sigma}+t)^{\zeta}) \ . \tag{71}$$

For large x, we must have $g(x)\sim x^{-\sigma}$ as determined by the $r\to\infty$ limit of $\bar{n}_2$, corresponding to a scaling solution for the distribution function

$$\bar{n}_2(r,t)\sim J(r,t) \ . \tag{72}$$

From (71) we see that this scaling form of $\bar{n}_2(r,t)$ will also be the solution for large t. This is consistent with the RG picture of an attractive fixed point which describes the asymptotically late-time dynamics for all initial distributions.

The solutions for $\bar{n}_2$ and Eq. (65) give two relations between the density and the distribution function. Using the small r limit of the distribution function, $\bar{n}_2(r,t)=r^{\sigma}t^{-\zeta}$, we get the equation

$$\frac{dn}{dt}=-2\zeta n^2 t^{\zeta-1} \ , \tag{73}$$

which is consistent with the scaling solution $n\sim t^{-\zeta}$. The amplitude is not correct, but the argument captures the qualitative features at least. Note that no system size dependence can appear in this approximation. For uncorrelated initial conditions the scaling solution for $\bar{n}_2$ is valid at $t=0$. Further qualitatively correct results may be obtained if we assume (72) holds for all t. Then the solution to (73) is

$$n(t)=\frac{n_0}{1+2n_0t^{\zeta}} , \tag{74}$$

which exhibits the asymptotic time dependence, and also the lack of n_0 dependence, we see in the simulations for $\sigma \geq 1$. In fact, under the same assumptions we can find $g(x)$ for all values of x for correlated initial conditions. Setting $t=0$ in (71) gives

$$g(x)=x^{-\sigma}\bar{n}_2(x,0) \tag{75}$$

from which it follows that

$$\bar{n}_2(r,t)=J(r,t)\bar{n}_2((r^{1+\sigma}+t)^{\zeta},0) . \tag{76}$$

Combining this with (65) gives

$$\frac{dn}{dt}=-2\zeta n^2 t^{\zeta-1}\bar{n}_2(t^{\zeta},0) , \tag{77}$$

which can be rewritten as

$$\frac{dn^{-1}}{dt^{\zeta}}=2\bar{n}_2(t^{\zeta},0) . \tag{78}$$

Thus the late-time behavior of the density is completely determined by the initial two-particle distribution function in this approximation. We can test (78) by introducing correlations into the initial conditions. In particular, if we generate a system via the nearest-neighbor distribution

$$P(x)=\begin{cases}\dfrac{1}{2n_0\Delta}, & n_0^{-1}(1-\Delta)<x<n_0^{-1}(1+\Delta)\\ 0 \quad \text{otherwise}\end{cases} \tag{79}$$

then $\bar{n}_2(r,0)$ will be sharply peaked around $r=n_0^{-1}$, less sharply peaked around $r=2n_0^{-1}$, and so on out to infinity where it is equal to 1. The first $k=(1+\Delta)/(2\Delta)$ peaks will have zeros between them, which implies $dn^{-1}/dt^{\zeta}=0$. Therefore we expect a plot of n^{-1} versus t^{ζ} to have flat areas separated by sharp jumps, like a staircase, with the jumps smoothing to a straight line at late times. The simulation results for these initial conditions (shown in Fig. 8) verify the staircase pattern. Both the truncation method developed here and the property of lack of dependence on initial conditions are reinforced by this result.

VI. SIMULATIONS

To simulate these systems we simply directly integrated the equations of motion

$$\dot{x}_i=\sum_{j\,(\neq i)}(-1)^{i+j}|x_j-x_i|^{-\sigma}\mathrm{sgn}(x_i-x_j) . \tag{80}$$

Whenever two charges pass each other they were removed from the system. We began with some number of charges N_0 distributed randomly along a length L. To reproduce periodic boundary conditions exact replicas of the charge configuration were made, and added to the left and the right of the original system. Then the forces were calculated on the original charges, the positions updated, and the replicas replaced with updated copies.

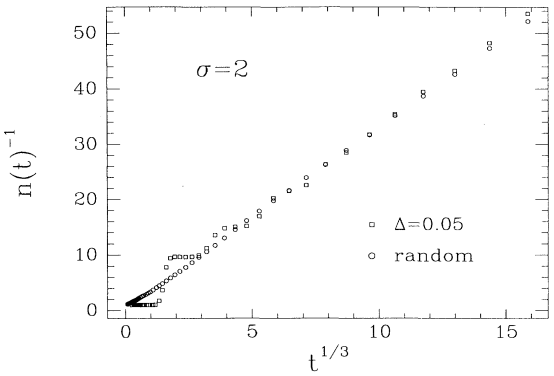

FIG. 8. Simulations for the correlated initial conditions discussed in the text, for $\sigma=2$, $\Delta=0.05$, and $N_0=100$. The data are plotted as n^{-1} versus $t^{1/3}$, which should give a staircase pattern as discussed in the text. The first three zeros of the slope are clearly visible. The data for the random initial conditions are plotted for reference.

While this emulates a periodic system, it also adds a long-range cutoff to the interactions. It is important to separate the effect of the cutoff from possible system size dependence effects.

We parametrized the cutoff in the following way. If k replicas are added to the left and to the right of the original system, there are $N_e=(2k+1)N(t)$ effective charges in the system. We imposed a minimum number of effective charges $N_{\min}$, and then determined the number of replicas needed so that $N_e \geq N_{\min}$. By comparing simulations with different values of $N_{\min}$, we could determine at what point the results are independent of the cutoff to our desired accuracy. We choose this method of introducing a cutoff, rather than a more obvious choice of including interactions out to a certain length, because otherwise small number effects entered into the simulations at late times. By keeping the effective number of charges at some minimum level we hoped to more accurately model the truly periodic system. The values we used for $N_{\min}$ are given in the table.

The numbers for $N_{\min}$ are large enough, particularly for $\sigma=\frac{1}{2}$, to significantly slow the simulations. Some speed can be regained by exploiting the insensitivity of the system to the time step. For $\sigma=\frac{1}{2}$ and $n_0=1$ we used an initial time step of $\Delta t=10^{-3}$, which we stepped up to $\Delta t=1$ over the time interval $t=(0,20)$ (for other values of σ see Table I). Although these values for the time step seem large, the results of the simulation are quite insensitive to the size. Simulations performed with ten times this step size showed no appreciable change. This is somewhat expected, since the primary consequence of a large time step is to cause the annihilating pairs to stay around longer, but the force exerted on the system by a very close pair of charges is nearly zero. It is probable that an even larger time step than the one used here would be adequate.

We used the second-order Runge-Kutta integration technique, which involves initially taking a half step, reevaluating the forces at this midpoint, then going back

TABLE I. Values of the simulation parameters used. For all simulations $n_0=1$ and $N_0=100, 200, 400, 800$. The time step is ramped from $10^{-3}\Delta t$ to Δt in the range $0<t<t_0$, and is equal to Δt for $t>t_0$.

	N_r	$N_{\min}$	Δt	t_0
$\sigma=\frac{1}{2}$	300	400	1	20
$\sigma=1$	1000	30	0.1	2
$\sigma=2$	1000	20	0.03	0.6

and taking a full step with the modified forces. To use this method it is necessary to check for annihilation at the midpoint, or else the forces calculated at the midpoint for a pair which has just passed each other will be quite inaccurate. It seems likely that using the Euler integration method instead of Runge-Kutta would give the same results.

The third parameter in the simulations is the number of runs over which the quantities are averaged. That is, since the quantities are supposed to be averaged over the distribution of initial conditions, we average over multiple runs. To determine the number of runs N_r over which to average, we calculated the standard deviation of $n(t)$ via the central limit theorem. For $\sigma=\frac{1}{2}$ we used $N_r=300$, for which the one-σ error bars were smaller than the point size of the plots for much of the scaling regime.

These simulations were performed on a DECstation 5000. Our goal was to use as simple an algorithm as possible, and to keep simulations at the level of a workstation problem. There are ways in which our techniques could be expanded or improved upon, for example, by using a controlled time step which maximally exploits the insensitivity of the system, or of course, by using faster computers. It would be preferable to push the $\sigma=\frac{1}{2}$ system to larger values of N_0, but this was where we were reaching our limits.

VII. DISCUSSION

The first of the principal results of this paper is the appearance of system size dependence in simulations for $\sigma=\frac{1}{2}$. We believe that this result also holds for all $0<\sigma\leq 1$ on the basis of our fugacity expansion, which demonstrates anomalous L dependence in the expansion coefficients for this range. The data for $\sigma=1$ exhibit only slight L dependence. However, the effect may be very small at the marginal value. This result could bear a more thorough scrutiny via simulations, particularly if data for larger system sizes can be generated.

The other principal result is the possibly more general dynamical feature of lack of dependence on the initial length scale. From a renormalization-group perspective this is an intuitive result: once the system has reached the fixed point, and is thus evolving in time via a rescaling of the domain length only, then the information about the path to the fixed point is lost. For the distributions we used, the information lost is the initial density and correlations. A variety of distributions may flow to this same fixed point, which can then be interpreted as a loss of information about the initial distribution itself, and not just its length scale. This is suggestive of a dynamical feature of lack of dependence on prequench temperature, if thermal distributions flow to the same fixed point. The RG picture is complicated by the presence of system size dependence, since the notion of a scale invariant fixed point will need modification. In the simulations we find a convincing lack of n_0 dependence for $\sigma=1,2$, and a possible lack of n_0 dependence for $\sigma=\frac{1}{2}$. We also find, via a heuristic argument (34), that the presence of L dependence should not affect the lack of dependence on the initial length scale.

Our theoretical approaches include the fugacity expansion and the truncation method of Sec. V. The latter approach is useful in providing a qualitative description of the dynamics, and includes quite naturally the dynamics at late times. In the former case, the original intent was to find results for the infinite system while calculating with finite L. We can find all the expansion coefficients for $\sigma=0$, and thus the exact answer for $n(t)$ (see Appendix C), but we find that the density decays exponentially. This indicates that $\sigma=0$ is singular in some sense, and that trying to expand about this solution is not likely to be fruitful. We can calculate the expansion coefficients to order y^4 by taking the large σ limit. This calculation can be carried to higher orders, the problem becoming an exercise in bookkeeping. When we attempt to extrapolate the large σ result to lower values of σ we find divergences appearing in our expansion coefficients. This is a general feature for $\sigma\leq 1$, the physical range of interest. These divergences are of the form of L-dependent expansion coefficients, whose presence may just be indicating system size dependence in the density $n(t)$.

Our expression for the density in the large σ limit can be used to calculate a Callan-Symanzik β function to order g_R^4. To this order the β function has a zero with the value $g_R^*=0.33$ which predicts the scaling function (21) has the asymptotic form

$$f(x)\sim 0.33x^{-1}\ . \tag{81}$$

This β function approach, while useful in giving a qualitative description of the fixed point, may not give a robust value for the coefficient of the asymptotic region. If we take the same $f(x)$ used to derive the β function and use the method of Padé approximants, we find for large x

$$f(x)\sim 0.15x^{-1}\ . \tag{82}$$

Unfortunately, we have not been able to find any analog of the ϵ expansion of the equilibrium critical behavior, which would allow a systematic truncation of the series for the β function.

The one-dimensional system with long-range interactions appears to have complicated behavior for $\sigma\leq 1$. These interactions appear to be relevant in higher-dimensional systems as well [5], suggesting that system size dependence may be a more general feature of long-range interacting systems. Simulations of these systems in higher dimensions, although difficult, could yield in-

teresting results. More can be done with the one-dimensional simulations in the way of measuring correlation functions as well. A theoretical approach which treats the system size dependence in a controlled way, perhaps some modification of our density expansion, would be a possible next step in trying to understand these systems.

ACKNOWLEDGMENTS

We thank A. Bray and A. Rutenberg for a useful correspondence. This work was supported by NSF Grant No. PHY 91-16964.

APPENDIX A: Q-STATE POTTS MODEL

We can generalize the Ising model Hamiltonian (1), which is the $Q=2$ Potts model, to the case of general Q. At each lattice site there is a variable s_i, which can be in one of the Q states. The Hamiltonian is defined by

$$H=-\sum_{\substack{i,j\\ i<j}} V(x_i-x_j)J(s_i,s_j) , \tag{A1}$$

where $V(r)$ is the same as before, and

$$J(s_i,s_j)=1-\delta_{s_i s_j} . \tag{A2}$$

We can rewrite the Hamiltonian as

$$H=\sum_{\substack{i,j\\ i<j}} U(x_i-x_j)[J(s_{i+1},s_{j+1})+J(s_i,s_j) -J(s_{i+1},s_j)-J(s_i,s_{j+1})] +(\text{surface terms}) , \tag{A3}$$

where the function $U(r)$ is defined by (4) [12]. Notice the expression in the square brackets is zero for $s_i=s_{i+1}$ or $s_j=s_{j+1}$. Therefore this term only contributes to the energy when x_i and x_j are both locations of defects. A defect can be labeled by (α,β), meaning it is the boundary between a region of state α and a region of state β. The interaction for a pair of defects of type (α,β) and (γ,β) separated by a distance r is then

$$H_{\text{pair}}=U(r)[\delta_{\alpha\gamma}+\delta_{\beta\delta}-\delta_{\alpha\delta}-\delta_{\beta\gamma}] . \tag{A4}$$

Consider a nearest-neighbor pair of defects. This implies $\beta=\gamma$, and we assume $\alpha\neq\delta$. The interaction energy is then

$$H_{\text{pair}}=-U(r) . \tag{A5}$$

Also note that if all four states $\alpha,\beta,\gamma,\delta$ are distinct then there is no interaction between the defects. Now we take the $Q\to\infty$ limit of this model. Every domain in the system will find a unique state, and so all defect pairs will have $\alpha,\beta,\gamma,\delta$ not equal, with the exception of nearest neighbors. These rules allow us to drop the designation of the states, and simply consider the model to be one where only nearest neighbors interact. The defect Hamiltonian can be written as

$$H=-\sum_i U(x_i-x_{i+1}) . \tag{A6}$$

We introduce the same equations of motion as before, with the consequence that now only the nearest neighbor on either side is included in calculating the force. There is another modification to the dynamics. When a nearest-neighbor pair annihilate, a single defect remains. That is,

$$(\alpha,\beta)+(\beta,\gamma)\to(\alpha,\gamma) . \tag{A7}$$

APPENDIX B: THREE-BODY PROBLEM FOR $\sigma=1$

We start by taking the L derivative of $Q_3(t)$, leading to the calculation in the (r_1,r_2) plane as shown in Fig. 7. We want to solve for the function which gives the time to first annihilation, $T(r_1,r_2)$. From this we can find $Q_3(t)$ via

$$\frac{\partial Q_3(t)}{\partial L}=-2\int_{r_1+r_2<L} dr_1 dr_2 \Theta(t-T(r_1,r_2)) . \tag{B1}$$

The time to annihilation has the scaling form

$$T(r_1,r_2)=r_2^2 f\left[\frac{r_1}{r_2}\right] . \tag{B2}$$

If r_1 and r_2 are evolved by a time δt, then T will change by $-\delta t$. That is, for $r=r_1/r_2$

$$T-\delta t=(r_2+\dot r_2\delta t)^2 f(r+\dot r\delta t) , \tag{B3}$$

so to order δt we get the equation

$$2r_2\dot r_2 f(r)+r_2^2\dot r f'(r)=-1 . \tag{B4}$$

The three-charge equations of motion given by (47) and the rescaling of time (17) give

$$\frac{1}{4}r_2\dot r_2=-2+\frac{r_2}{r_1}+\frac{r_2}{r_1+r_2} =-2+\frac{1}{r}+\frac{1}{r+1} \tag{B5}$$

and

$$\frac{1}{4}r_2^2\dot r=r_2\dot r_1-r_1\dot r_2 =-\frac{2}{r}+2r+\frac{1}{r+1}-\frac{r}{r+1} . \tag{B6}$$

Therefore r_2 can be eliminated from Eq. (B4), giving the differential equation for $f(r)$,

$$\frac{2(1-2r^2)}{(r-1)(2r^2+3r+2)}f(r)+f'(r) =\frac{-4r(r+1)}{(r-1)(2r^2+3r+2)} . \tag{B7}$$

Notice that the coefficients are singular at $r=1$.

This equation can be integrated in closed form, which is somewhat surprising, with the result

$$f(r)=\tfrac{4}{3}(1+r+r^2)+C(r-1)^{2/7}(2r^2+3r+2)^{6/7} , \tag{B8}$$

where C is a constant of integration. To determine C we

consider the large r limit of $f(r)$. If $r_1 \gg r_2$ then the time to annihilation is given by the separation r_2 only, and is $T=r_2^2$. This implies for large $r, f(r)=1$. If we choose as our integration constant $C=-2^{8/7}/3$, then the r^2 and r parts of $f(r)$ have coefficients of zero. Therefore the exact solution is

$$f(r)=\frac{4}{3}(1+r+r^2) - \frac{2^{8/7}}{3}(r-1)^{2/7}(2r^2+3r+2)^{6/7} . \tag{B9}$$

When we plot $T(r_1,r_2)$ on the (r_1,r_2) plane (see Fig. 7) we see a cusp at $r_1=r_2$. The appearance of the exponent 1/7 is curious. When we use this solution to calculate the area between the $\sigma=1$ and the large σ curves, we find this area is divergent, as mentioned in the text.

APPENDIX C: $\sigma=0$ SOLUTION

For the $\sigma \to 0$ limit of the model we have the equations of motion

$$\dot{x}_i = -\frac{\partial}{\partial x_i} \sum_{\substack{j,k \\ j<k}} (-1)^{j+k}|x_j - x_k| = \sum_{k\ (\neq i)} (-1)^k \mathrm{sgn}(i-k) . \tag{C1}$$

The force on a given charge does not depend on the position of its neighbors, only on the global excess of charge on either side. It is necessary to consider only systems with even numbers of charges, since a system with an odd number of charges will have all forces equal to zero. For an even charge system the charges will be attracted in isolated pairs. That is, the leftmost charge, call it positive, will see a net negative charge to the right. The second charge from the left will be negative and see only a net positive charge to the left. This pair will then move toward each other an annihilate independent of the rest of the system.

The time-dependent density in this model is entirely determined by the probability distribution for the location of the nearest neighbors. For the random initial conditions we used, this is a Poisson distribution

$$P(x)dx = n_0 e^{-n_0 x} dx , \tag{C2}$$

where $P(x)dx$ is the probability of the nearest neighbor being located between x and $x+dx$. At a given time t all the paired charges which are located within a range $\Delta x(t)$ will have annihilated. For the rescaled time given by (17)

$$\Delta x(t) = t . \tag{C3}$$

The fraction of initial charges which remain at time t is then

$$\frac{n(t)}{n_0} = 1 - \int_0^t dx\, n_0 e^{n_0 x} = e^{-n_0 t} \tag{C4}$$

so the density scaling function (21) is

$$f(x) = e^{-x} . \tag{C5}$$

This result can be found also by using the fugacity expansion for $\sigma=0$.

*Present address: Department of Physics, Theoretical Physics, 1 Keble Road, Oxford OX1 3NP, England.

[1] J. D. Gunton, M. San Miguel, and P. S. Sahni, in *Phase Transitions and Critical Phenomena,* edited by C. Domb and J. L. Lebowitz (Academic, New York, 1983), Vol. 8, p. 267; K. Binder, Physica A **140**, 35 (1986); H. Furukawa, Adv. Phys. **34**, 703 (1985).

[2] A. J. Bray, Phys. Rev. Lett. **62**, 2841 (1989); Phys. Rev. B **41**, 6724 (1990).

[3] I. M. Lifshitz, Pis'ma Zh. Eksp. Teor. Fiz. **42**, 1354 (1962) [Sov. Phys. JETP **15**, 939 (1962)]; S. M. Allen and J. W. Cahn, Acta Metall. **27**, 1085 (1979).

[4] M. K. Phani *et al.*, Phys. Rev. Lett. **45**, 366 (1980); P. S. Sahni *et al.*, Phys. Rev. B **24**, 410 (1981).

[5] A. J. Bray and A. D. Rutenberg (unpublished); H. Hayakawa, Z. Rácz, and T. Tsuzuki, Phys. Rev. E **47**, 1499 (1993).

[6] R. J. Glauber, J. Math. Phys. **4**, 191 (1963).

[7] F. J. Dyson, Commun. Math. Phys. **12**, 91 (1969); **12**, 212 (1969).

[8] A. J. Bray, J. Phys. A **22**, L67 (1989).

[9] K. G. Wilson and J. Kogut, Phys. Rep. **12**, 75 (1974).

[10] See, for example, D. J. Amit, *Field Theory, the Renormalization Group, and Critical Phenomena* (World Scientific, Singapore, 1984), p. 189 ff.

[11] P. C. Hohenberg and B. I. Halperin, Rev. Mod. Phys. **49**, 435 (1977).

[12] J. L. Cardy, J. Phys. A **14**, 1407 (1981).